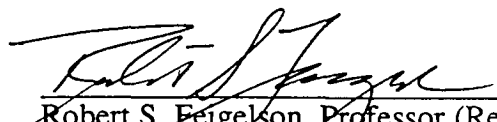


The Board of Trustees of the
Leland Stanford Junior University
Center for Materials Research
Stanford, California 94305-4045
Santa Clara, 12th Congressional District

Annual Technical Report
on
PROTEIN CRYSTAL GROWTH IN LOW GRAVITY
NASA #NAG8-774
CMR-90-5
SPO#7218
for the period
April 27, 1989 through April 26, 1990

Submitted to
George C. Marshall Space Flight Center
ES-76, Space Science Lab
MSFC, AL 35812

Principal Investigator:


Robert S. Feigelson, Professor (Res.)
Center for Materials Research
Stanford, California 94305-4045
(415) 723-4007

June 1990

TABLE OF CONTENTS

ABSTRACT	1
I. INTRODUCTION	1
II. FLUID FLOW	2
III. ISOCITRATE LYASE	3
IV. PRELIMINARY CONTROLLED NUCLEATION EXPERIMENTS	5
V. CONTROLLED NUCLEATION APPARATUS	5
VI. CONTROLLED NUCLEATION EXPERIMENTS	6
VII. GROWTH OF LYSOZYME BY TEMPERATURE GRADIENT (ΔT)	7
VIII. REFERENCES	9
IX. FIGURES	10

ABSTRACT

This report covers the period of April 27, 1989 to April 26, 1990 for NASA Grant NAG 8-774. The objectives of and approach to the research is outlined. The further analysis of the flows around growing crystals is detailed. The preliminary study of the growth of isocitrate lyase, the crystal morphologies found and the preliminary x-ray results are discussed. The design of two apparatus for protein crystal growth by temperature control are presented along with preliminary results.

I. INTRODUCTION

The objective of this research is to study the effect of low gravity on the growth of protein crystals and those parameters which will affect growth and crystal quality. The proper design of the flight hardware and experimental protocols are highly dependent on understanding the factors which influence the nucleation and growth of crystals of biological macromolecules. Thus, the primary objective of this research is centered on investigating those factors and relating them to the body of knowledge which has been built up for "small molecule" crystallization. This data also provides a basis of comparison for the results obtained from low-g experiments.

The main component of this research program is the study of mechanisms involved in protein crystallization and those parameters which influence the growth process and crystalline perfection. Both canavalin and lysozyme are being used as the basic model proteins in these studies. Other biological macromolecules such as isocitrate lyase have been included in this research program when they provide an opportunity to better understand the nature of the crystallization process. The program involves four broad areas:

1. The application of both classical and novel chemical and physical techniques to study the fundamentals of protein crystallization. Included in this area are the study of the phase relationships in the systems of interest, primarily the factors controlling solubility, the study of growth kinetics to determine the growth rate controlling mechanism and the relevant activation energy involved in the process. The effects of fluid flow on the growth and perfection of protein crystals will be studied using flow visualization techniques. The use of electrochemical techniques to monitor and/or control crystallization will be studied also. The effects of applied

voltages on nucleation and growth are not known nor is the magnitude of the potentials which may develop on the crystal during growth.

2. Characterization of protein crystals. Optical microscopy will give a general evaluation of crystal morphology, size and perfection. Phase contrast techniques will give enhanced contrast to the surface features allowing observation down to the 0.1μ level. For more detailed surface imaging the application of Scanning Tunneling Microscopy and Atomic Force Microscopy to protein crystals will be investigated. To study the defects occurring in the bulk of the crystals, the applicability of Synchrotron x-ray topography will be studied. The characterization studies will be attempting to associate the defects in protein crystals with the growth conditions to develop insights for growing crystals of greater perfection.
3. Control of nucleation and growth. The information developed in the phase relationship studies of section 1) will be used to design experiments to separately control the nucleation and growth processes. The information from section 2) will be used to optimize the growth.
4. The design and construction of a prototype of space flight hardware. The design will incorporate the results of section, 3) and will be instrumented to gather the types of data that have been acquired in the ground based studies.

II. FLUID FLOW

The analysis of the flows around growing crystals has been expanded. In a previous report,⁽¹⁾ it was noted that flows had been observed around growing crystals of Rochelle salt, lysozyme and canavalin using the Schlieren imaging technique (Fig. 1). The values for the change of density and index of refraction with change of concentration for each system were also reported. The change in density and index of refraction with concentration do not by themselves indicate whether flow will occur and, if it does, whether that flow can be imaged. The Grashof number,

$$Gr = \frac{g\Delta\rho}{\rho\nu^2} L^3$$

(g is the acceleration of gravity, $\Delta\rho$ the change in density across the diffusion boundary layer, L the characteristic length of the system-taken to be the height of the crystal, ρ the density and ν the viscosity) is a non-dimensional, fluid dynamic variable that relates the buoyant force to the viscous drag. The larger this number, the more likely that flow will occur. More importantly, systems with the same Grashof number should behave alike.

Thus, if a range of values of Grashof numbers can be established over which flow can be demonstrated to occur in crystallizing systems, then calculation of a Grashof number for a new system (macromolecular or not) will predict if flow should occur in that system.

Similarly, the ability to image the flow is not directly dependent on the change of index of refraction with concentration, but is related to the local change in light intensity

$$\Delta I/I = (f_2/a) \int (1/n) (\partial n/\partial x) dz$$

where f_2 is the focal length of the second mirror in the schlieren optics, a the knife edge aperture, n the index of refraction, $\partial n/\partial x$ is given by $(dn/dc)(\partial c/\partial x)$ where x is the direction across the plume, and dz is perpendicular to the plan of the film. Again it should be possible to establish a range of values under which the flows will be visible. Comparisons of new systems will establish the possibility of flow visualization.

In addition to the values for the changes in density and index with concentration, it is necessary to establish the actual concentration at the crystal interface. For a crystal growing under diffusion control (Rochelle salt), it is equal to the solubility. However, lysozyme⁽²⁾ and canavalin⁽³⁾ grow under interface control and the interface concentration may be estimated by using a method outlined by Pusey and Naumann.⁽⁴⁾ Using these estimates, the Grashof number and the local change in light intensity for each system have now been calculated under the experimental conditions used. The values of the Grashof number are 772.48 for Rochelle salt, 23.04 for lysozyme and 67.84 for canavalin. If the Grashof number is normalized by fixing the size of the crystals at 1mm, then the Grashof numbers become 112.64 for Rochelle salt, 7.04 for lysozyme and 8.96 for canavalin. There is a much lower tendency for the protein solutions to experience convection under the conditions of these experiments even when size considerations are taken into account, but flow does occur in all these systems. The values found for the local change in light intensity are 21.7 for Rochelle salt, 2.93 for lysozyme and 4.39 for canavalin. Based on the image quality of the films used in this study, the value of 2.39 appears to be near the limit of detectability in our system (400ASA film, f2.8, 1/51 sec exposure).

III. ISOCITRATE LYASE

A study of the growth behavior of isocitrate lyase has recently begun. This is a joint project with Du Pont. When grown by the hanging drop method on earth, the crystal grows in a manner such that the corners grow out rapidly and the crystal quality is poor. Crystals grown in space however are equiaxed. Crystals of this material have been grown

in our laboratory by the hanging drop method. The solutions used in this and subsequent growths were: a protein solution of 0.1ml of 13mg/ml isocitrate lyase with 0.004ml of a solution of 5.95mg of 3-nitropropionate and 107.23mg of magnesium acetate in 1ml of 50mM Tris (pH 7.0) and 0.004ml of a solution of 15.36mg of glutathione and 3.72mg of disodium EDTA in 0.15ml of 1M Tris (pH 8.0) (final protein concentration was 12mg/ml), and a well solution consisting of 72% saturated sodium citrate and containing 30mM Tris at pH 8.3. The drop was made up of 2 μ l of the protein solution and 2 μ l of the well solution. The morphology of these crystals (Fig. 2 & 3) duplicates that of those produced at Du Pont. The growth rates were measured and, consistent with the morphology, the growth rate of the corners is initially high (1.8 microns/min) while that across the face center of the crystal is about 0.7 (Fig. 4 and 5). The growth rate of the corners remains above 0.2 microns/min for at least 1100 minutes while the face velocity drops essentially to 0 after 300 minutes. In order to test whether fluid flow was responsible for this unstable growth, a vapor equilibrium cell was built to allow flow visualization (Fig. 6). The cell volume was 20 μ l (5 times the volume of the 1-g hanging drop, 0.5 the volume of the space experiment). The cross section was 3mm x 1mm giving a surface area for equilibration which was 1/3 of that of the hanging drops. The crystals grown in this cell were, surprisingly, equiaxed (first time in a ground based experiment) with a similarity to the space grown crystals (Fig. 7). No flow data has been collected yet.

Additional growth experiments have been conducted in 2mm diameter capillary tubes. In these experiments 10 μ l of protein solution and 10 μ l of well solution are placed in the capillary and equilibrated against the well solution in a larger tube attached to the capillary. These experiments have not duplicated the results of the the growth in the Schlieren cell, but crystals of two different morphologies were found (Fig. 8 & 9). A total of four different crystal morphologies have been seen in our laboratory. The predominant morphology observed has a cross section that appears to be a flattened hexagon. The end of the "hexagon" terminate in a wedge shape. This morphology is consistent with the orthorhombic symmetry of the isocitrate lyase unit cell ($a=80.7\text{\AA}$, $b=123.1\text{\AA}$ and $c=183.4\text{\AA}$)(5) with slow growing faces bounded by low index planes. A variation of this morphology was found in the crystals with the enhanced corner growth. The instability in growth occurs at the corners of the terminal faces of the "hexagonal" form.

The third morphology which was found were thin platelets of about 5m thickness. These platelets were four sided with apex angles of $82.5\pm 1^\circ$ and $98.1\pm 0.5^\circ$. This morphology is not readily explained by the orthorhombic symmetry and low index slow

growth planes. The final morphology observed was the equiaxed crystals previously mentioned. There is not enough information to completely describe their morphology.

Recent x-ray studies at DuPont show that the "dendritic" crystals grown in 1-g, the crystals grown in space and the "hexagonal" crystals grown in the capillaries all belong to the same orthorhombic space group - $P2_12_12_1$.⁽⁶⁾ There is also some indication of slight changes in the unit cell parameters among these crystals.

Preliminary results show that the morphology of the isocitrate lyase crystals is not due to the sedimentation effect. Morphological stability seems to be related to the rate of equilibration of the protein solution and the crystal growth rate. Baird's work⁽⁷⁾ shows that hanging drops equilibrate faster in 1-g than in space and the reduced surface area of the flow cell guarantees a slower equilibration. This is borne out by the lower nucleation and growth rates observed in the flow cell and the capillaries.

The results of the space flight experiments carried out by DuPont give some indication that "aging" of the protein solution before crystallization may have an effect on the morphology of the crystals grown from that solution.⁽⁶⁾ This effect will be studied further in our laboratory.

IV. PRELIMINARY CONTROLLED NUCLEATION EXPERIMENTS

The solubility diagrams of both lysozyme⁽⁸⁾ and canavalin⁽⁹⁾ show a temperature dependence of the solubility. Based on this knowledge, preliminary controlled nucleation experiments using lysozyme have been conducted. These initial experiments used a small, temperature controlled spot to induce nucleation at a fixed position and to limit the number of nuclei produced. These experiments used lysozyme (20mg/ml, pH 4.0, 0.1M sodium acetate, and 4% sodium chloride). This solution will spontaneously nucleate in 4-5 days at room temperature. By using a cold spot temperature of 9° C, nucleation was accomplished in 5 hours. The number of nuclei was less when compared to the isothermal solutions, but they were not localized to the extent anticipated (Fig. 10).

V. CONTROLLED NUCLEATION APPARATUS

The results of the preliminary localized nucleation experiments has led to the design and construction of the first prototype space flight hardware. This design incorporates a more sophisticated localized temperature gradient control as well as a means of controlling

the ambient temperature around the growth cell as an aid to localizing the nucleation as well as a means of controlling subsequent growth. The apparatus (called the Thermonucleator) also has provisions for in situ microscopy, the inclusion of schlieren optics, and the optical detection of the onset of nucleation (Fig. 11). The actual apparatus is shown in Fig. 12.

The thermal environment in the cell was probed using a thermocouple mounted on a x-z positioner. With this device, temperatures could be measured across the cell at various heights above the bottom. A set of profiles taken with the temperature surrounding the cell set at 25° C and the cold spot set at 15° C is shown in Fig. 13. The resulting isotherms are plotted in Fig. 14. Two features should be noted in these figures (13 and 14). The bottom is warmer than the adjacent layer at 0.04mm at distances greater than 0.4cm from the cold spot. This is due to thermal convection in the volume above the cold spot and stagnation in these warmer regions. Second, the cold spot temperature is lower than the set temperature due to the position and type of thermocouple chosen for the control thermocouple. This will be changed in the near future. The measured vertical temperature gradient above the cold spot is about 200° C/cm.

VI. CONTROLLED NUCLEATION EXPERIMENTS

The Thermonucleator has been tested using water, Rochelle salt and lysozyme. In some of the tests the ambient temperature was changed to increase the growth rate. The efficacy of this approach is shown in Fig. 15 which shows the continued growth of a canavalin crystal which had ceased to grow due to low supersaturation when the supersaturation was increased by changing the temperature from 22° C to 17° C.

Figure 16 shows the growth of an ice crystal from water. The exact spot temperature is not known. The initial growth of the crystal was extremely rapid and it was difficult to find the initial nucleus. After the crystal reached its maximum size, the cold spot was warmed and the crystal allowed to melt back. The last picture in figure 16 shows a small ice crystal produced in this manner sitting on the cold spot. This crystal could be maintained indefinitely. The pictures in this figure and the two subsequent figures were taken from the monitor screen of the time lapse video apparatus.

The next material to be grown in the Thermonucleator was Rochelle salt. The initial solution was made by dissolving Rochelle salt in hot water and allowing the solution to equilibrate with seed crystals producing a saturated solution at 24° C. 1cc of this solution was placed in the cell of the apparatus with the ambient temperature set at 24° C and the cold spot at 16° C. The experiment was started at 11:11am and, as seen in

Fig. 17, a crystal was visible at 1:29 pm. 8min later the crystal has grown to approximately 1mm in length. The cold spot temperature was then raised to the ambient temperature which had been lowered to 22° C to enhance the growth rate. In an hour, the crystal had grown to several mm in length and approximately 1mm high. Finally the ambient temperature was lowered to 20° C and the crystal allowed to grow for another 3 hours producing the crystal seen in the last picture in Fig. 17. There is a second crystal growing in the cell that was not nucleated on the cold spot. It is due to particles in the cell.

The final material in this test series was lysozyme. A saturated solution at 25° C was prepared using Pusey's solubility data.⁽⁸⁾ The composition of the solution was 58mg/ml lysozyme, 0.1M sodium acetate, 2% sodium chloride at pH4.0. The enclosure temperature was 25° C and the cold spot 15° C. The experiment was started at 9:49 am and the first crystals appeared at 2:18 pm (Fig. 18); a somewhat longer incubation time than that for the Rochelle salt. As seen in the subsequent pictures (Fig. 18), the growth rate of lysozyme is much slower than Rochelle salt. Lowering the temperature does increase the growth rate, but the final "crystal" is a polycrystalline mass. This strongly points out the need of a means to detect the early stages of nucleation so that the cold spot temperature can be raised to limit the number of nuclei (close examination of the first picture in figure 18 indicates that several nuclei were present). Future plans include the investigation of methods to accomplish this early detection of nucleation.

VII. GROWTH OF LYSOZYME BY TEMPERATURE GRADIENT (ΔT)

If a crystallizing material has a solubility which is dependent on temperature, then crystals can be grown by the transport of the material due to a temperature gradient. This is illustrated in Fig.19. The left side of the figure is a temperature profile such that the temperature at x is T and at $x+\Delta x$ it is $T+\Delta T$. When these temperatures are transferred to the solubility graph on the right of Fig. 19, they result in concentrations of c and $c+\Delta c$. The excess concentration, Δc , will cause material to diffuse to the colder region where it is incorporated in the growing crystal. This process will continue as long as there is a source of material at the warm end to replenish that which has been incorporated in the growing crystal. The results are shown schematically at the bottom of Fig.19. This analysis applies to materials which show normal solubility vs temperature behavior. For a material exhibiting retrograde solubility, the material would move from the cooler region to the warmer.

Lysozyme below 30° C exhibits a normal solubility vs temperature behavior⁽⁸⁾ and was chosen to test the feasibility of growing protein crystals by the temperature gradient method. The cell designed for this experiment is shown in Fig. 20. It consists of two microscope slides separated by a 0.0625 in spacer. The end temperatures were maintained by circulating water from temperature controlled baths through the ends. A uniform gradient was assured by the copper plate under the cell. The temperature gradient used and the resulting solubility profile are shown in Fig. 21. Figure 22 is the size of the crystal versus time. The initial growth rate was 0.56 μ /hr which was about 10% higher than was predicted by Pusey and Naumann's data⁽⁴⁾ when the high and low temperature solubilities were used to calculate the supersaturation. The growth rate drops to less than half the initial value (0.24 μ /hr) when the crystal reaches about 1050 μ in size. The reason for this behavior is unclear and it maybe related to the "terminal size effect".

Figure 23 shows the resultant crystal photographed in transmitted light with crossed polarizers. The initial seed crystal appears a light rectangle within the crystal. The pictures show both the extensive secondary nucleation which took place and the surface structure which developed on the growing crystal.

One possible explanation for the secondary nucleation seen in Fig. 23 was that small particles of lysozyme were drifting down from the source material and growing in the cooled regions. In order to prevent this, the cell was modified with baffles as shown in Fig. 24 which also shows the positions of the growing crystals. The temperature gradient and solubility profile of this cell was slightly different (Fig. 25). The growth behavior of two of the crystals is plotted in Fig. 26. They exhibit different growth rates (0.35 μ /hr and 0.27 μ /hr) and both of these rate are below that which would be predicted (0.44 μ /hr). One explanation for this is that in the first case the crystal was growing under the control of interface kinetics and in the second case there is mixed interface and diffusion control.

Figure 27 shows two of the crystal grown in the baffled cell. It is obvious that the baffles have not solved the problem of secondary nucleation.

As illustrated in Fig. 28, the analysis of the growth in a temperature gradient involves a large number of variables. The parameters effecting the solubility of the protein such as salt concentration, pH and buffers have not been included in this list but will be studied with the other parameters.

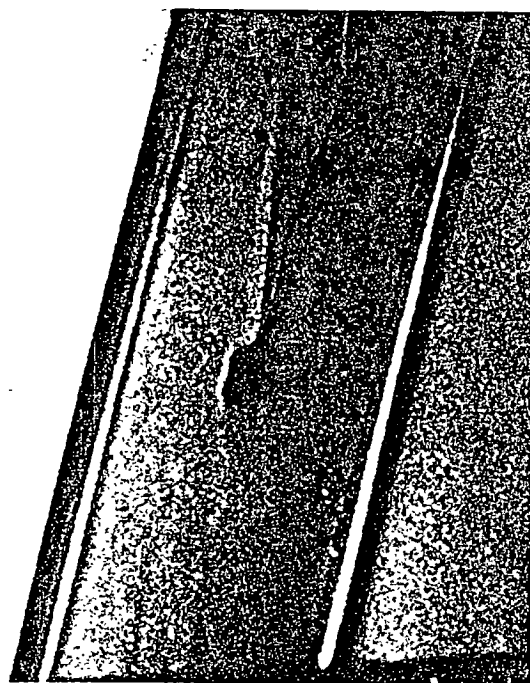
VIII. REFERENCES

1. Final Report "Protein Crystal Growth in Low Gravity", NASA Grant NAG 8-489.
2. S. Durbin, Proceedings of Third Intn'l Conf. on the Crystallization of Biological Macromolecules, 13-19 August, 1989, Washington, D.C.
3. R. De Mattei and R. Feigelson, *J. Crystal Growth* 76, 333 (1989).
4. M. Pusey and R. Naumann, *J. Crystal Growth* 76, 593 (1986).
5. L. DeLucas, Private communication.
6. P. Weber, Private communication.
7. J. Baird with W. Fowles, L. DeLucas, P. Twigg, S. Howard and E. Meehan, *J. Crystal Growth* 90, 117 (1988); with L. Sibilie, proceedings of Third Intn'l Conf. on Crystallization of Biological Macromolecules, 13-19 August, 1989, Washington, D.C.
8. M. Pusey, Private communication.
9. R. De Mattei and R. Feigelson, *J. Crystal Growth*, in submission.



Rochelle Salt

Lysozyme



Canavalin

Pictures oriented with flows vertical.

Fig. 1. Schlieren images of growth induced flow in Rochelle salt, lysozyme and canavalin.

ORIGINAL PAGE IS
OF POOR QUALITY

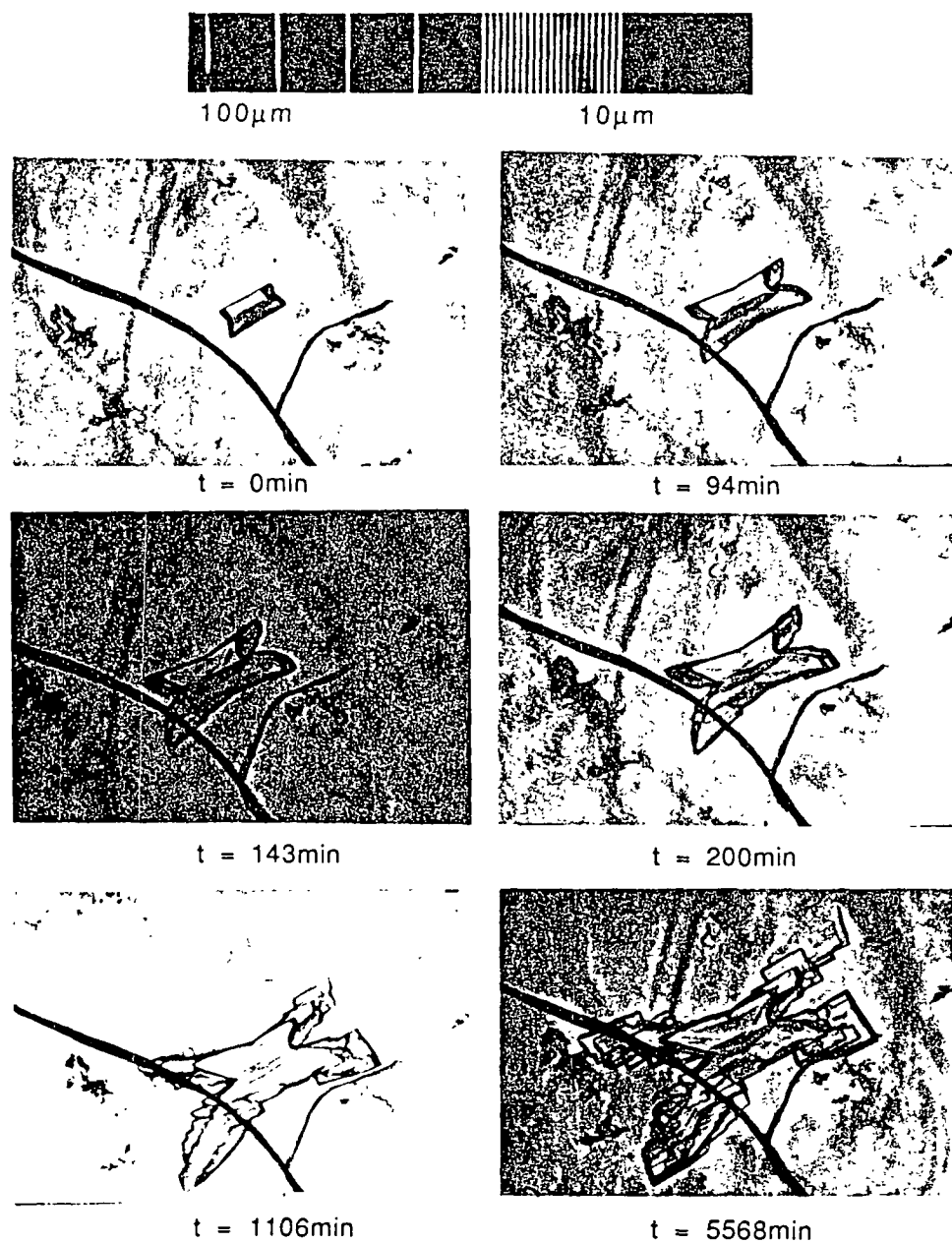


Fig. 2. Isocitrate lyase crystal grown by the hanging drop method at 1-g.

ORIGINAL PAGE IS
OF POOR QUALITY

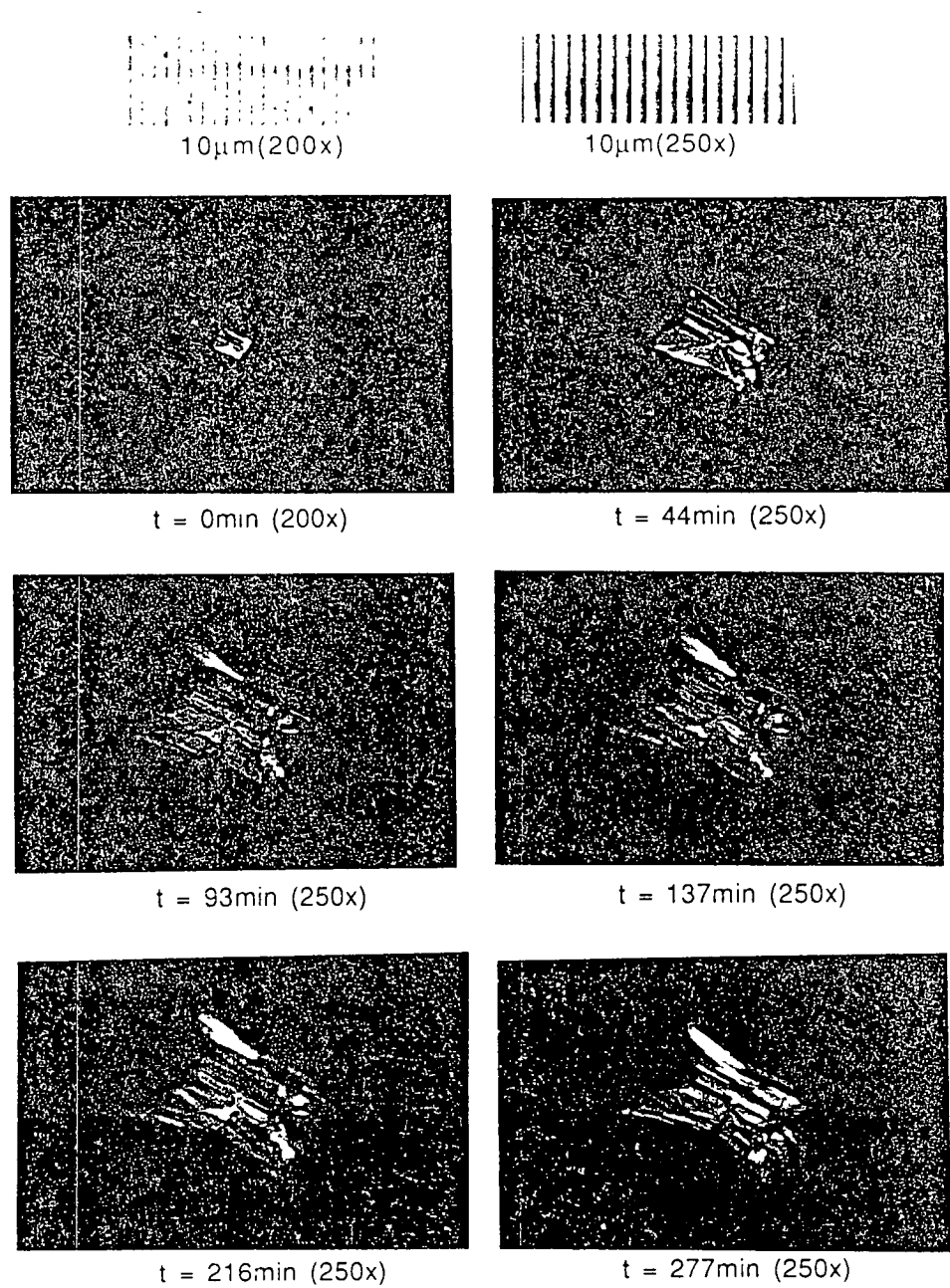


Fig. 3. Nomarski contrast micrographs of an isocitrate lyase crystal showing surface morphology.

ORIGINAL PAGE IS
OF POOR QUALITY

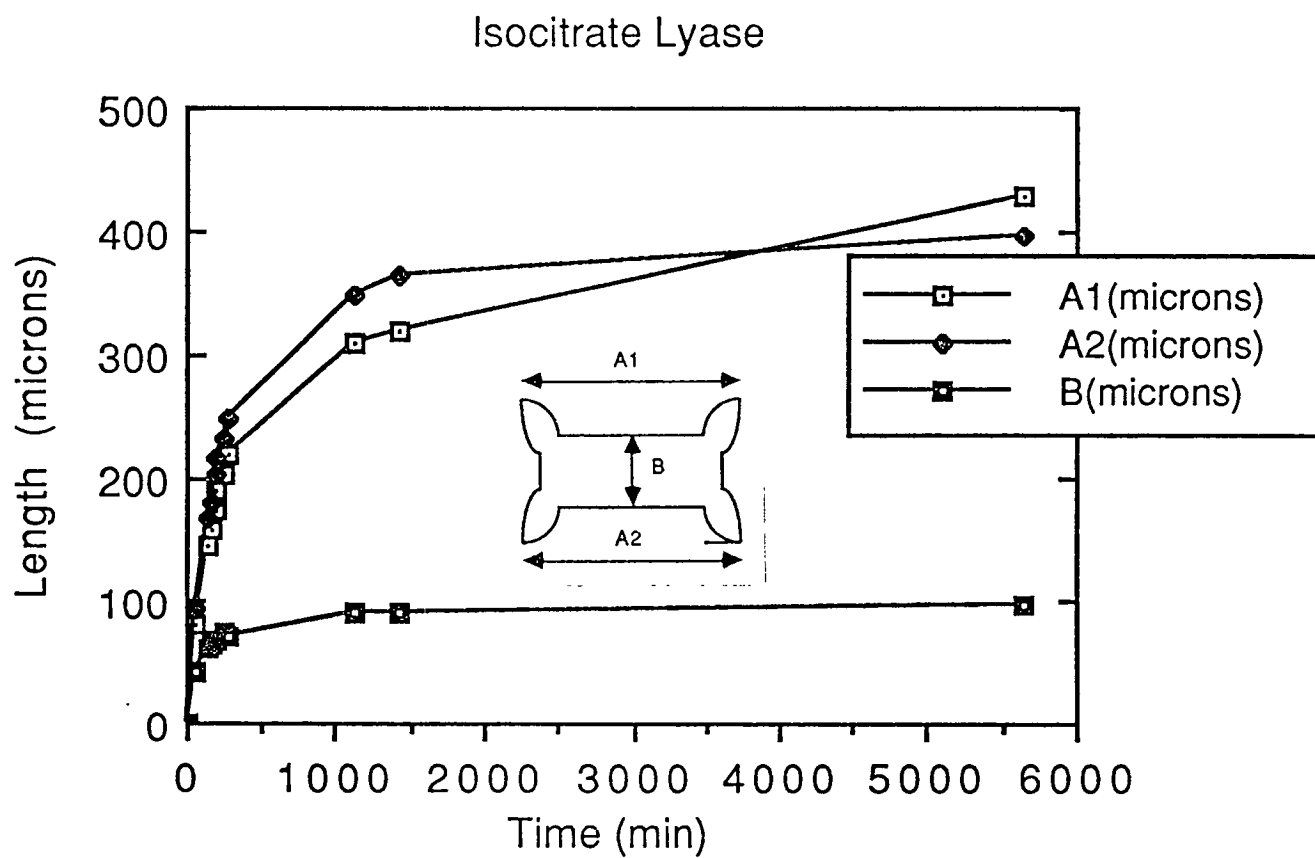


Fig. 4. Length versus growth time for crystal shown in Fig. 2.
T=0 is arbitrary.

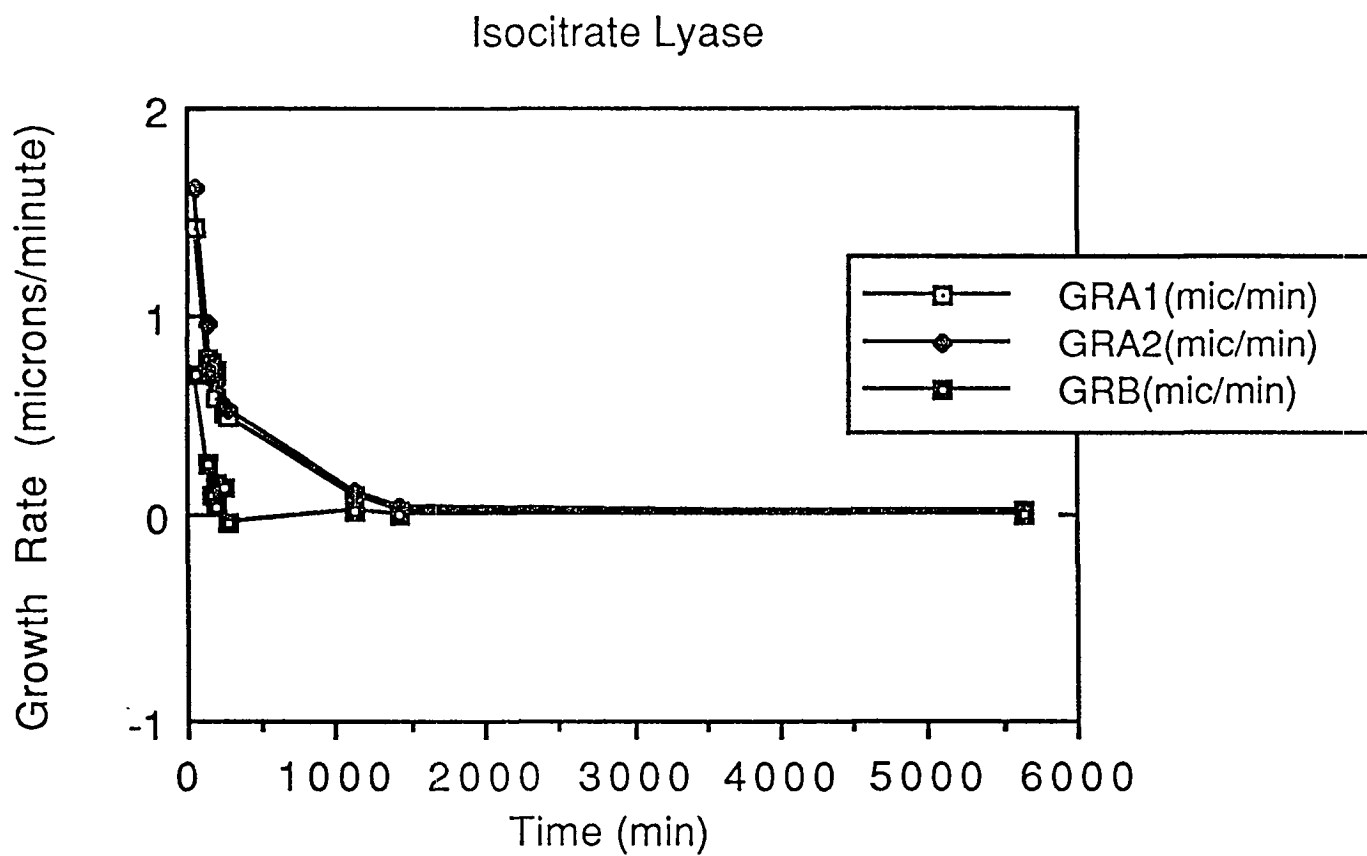


Fig. 5. Growth rate versus time for crystal shown in Fig. 2.

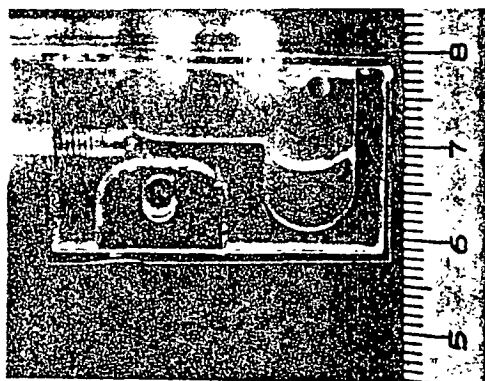
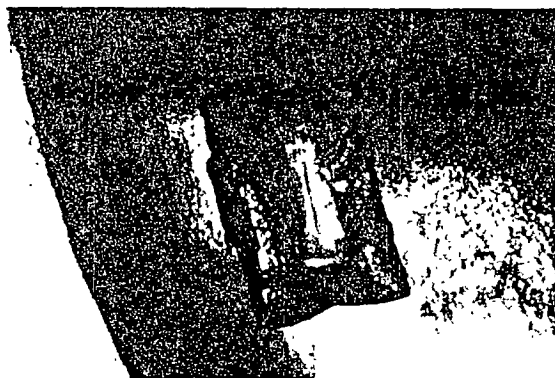


Fig. 6. Double well vapor diffusion cell.

ORIGINAL PAGE IS
OF POOR QUALITY



Grown near surface of solution



Grown near bottom of well

Fig. 7. Isocitrate lyase crystals grown in double well cell.

ORIGINAL PAGE IS
OF POOR QUALITY

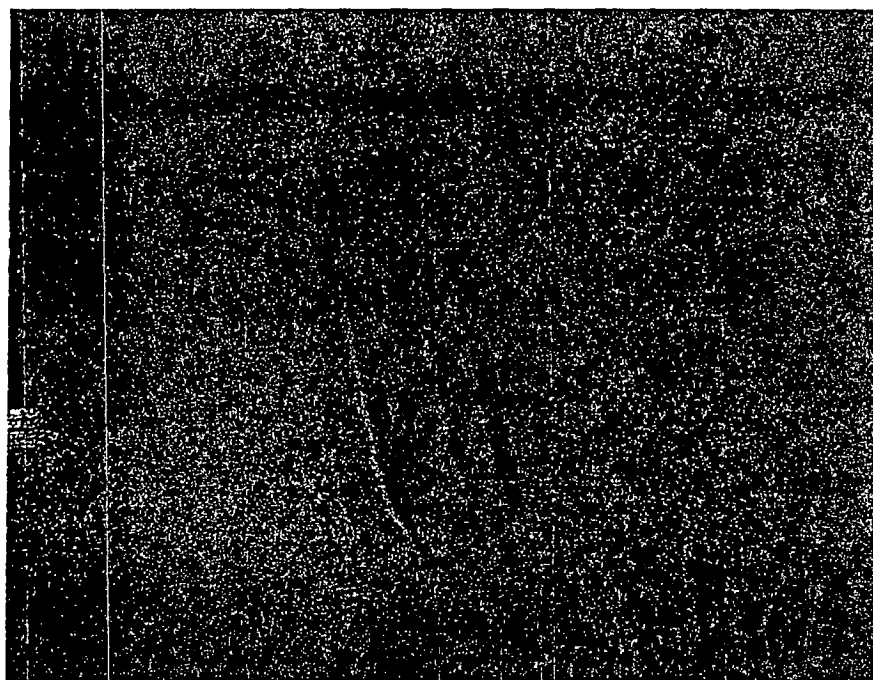


Fig. 8. Hexagonal-like isocitrate lyase crystals grown in capillaries.
200x

ORIGINAL PAGE IS
OF POOR QUALITY

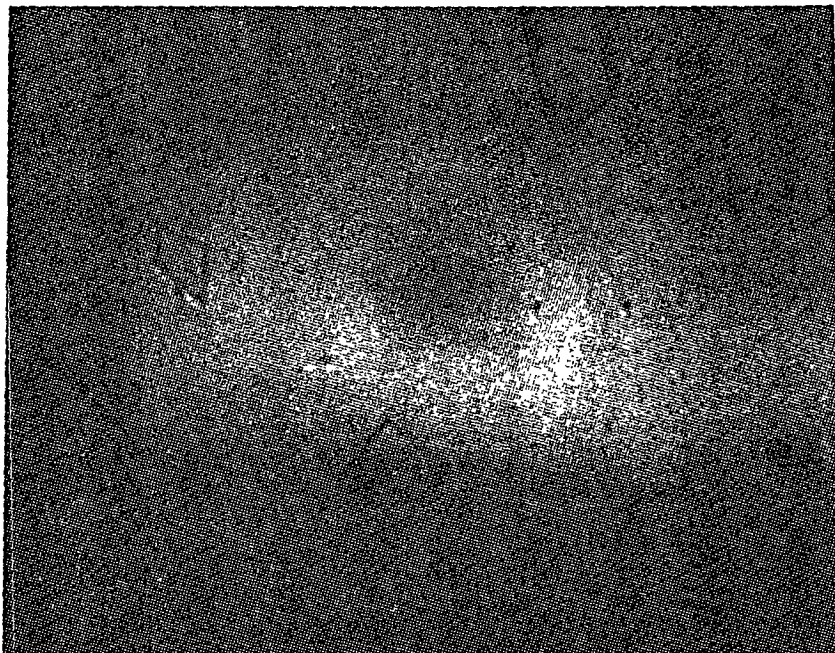
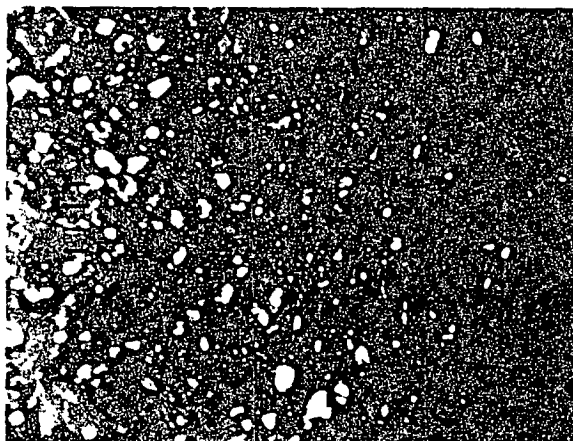


Fig. 9. Plate-like crystals of isocitrate lyase grown in capillaries.
200x

ORIGINAL PAGE IS
OF POOR QUALITY

UNCONTROLLED NUCLEATION



TEMPERATURE INDUCED
NUCLEATION

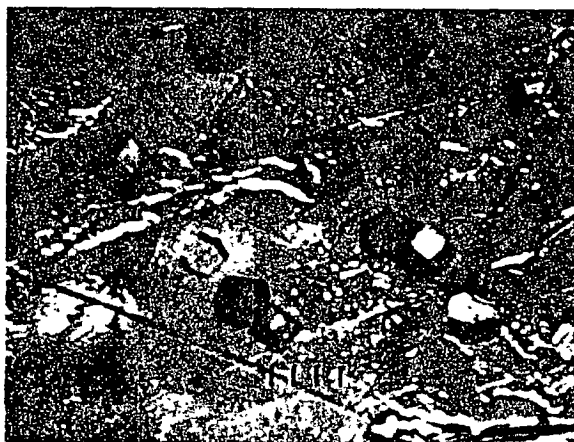


Fig. 10. Comparison of spontaneously nucleated and temperature nucleated lysozyme crystals. Index spacing is 100 μ .

THERMONUCLEATOR

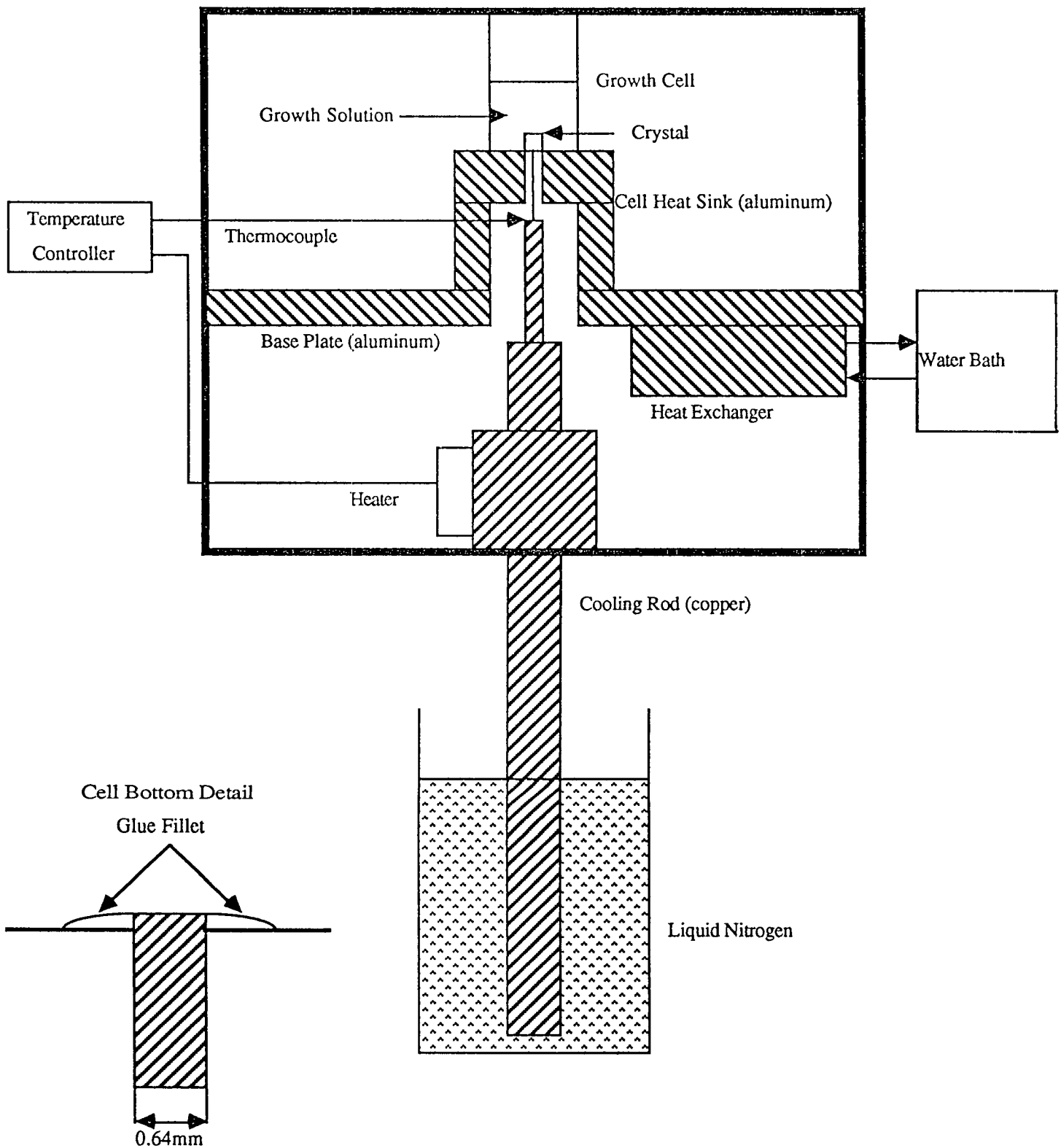
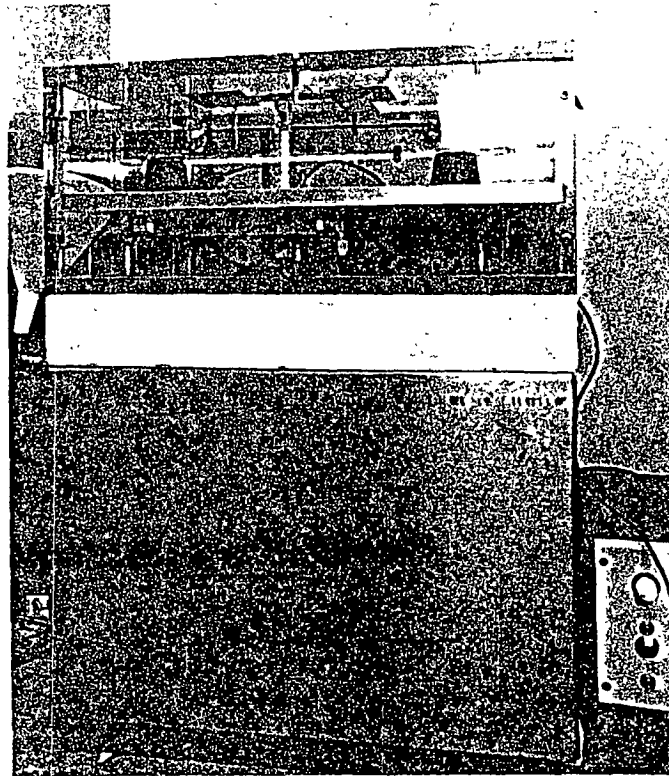
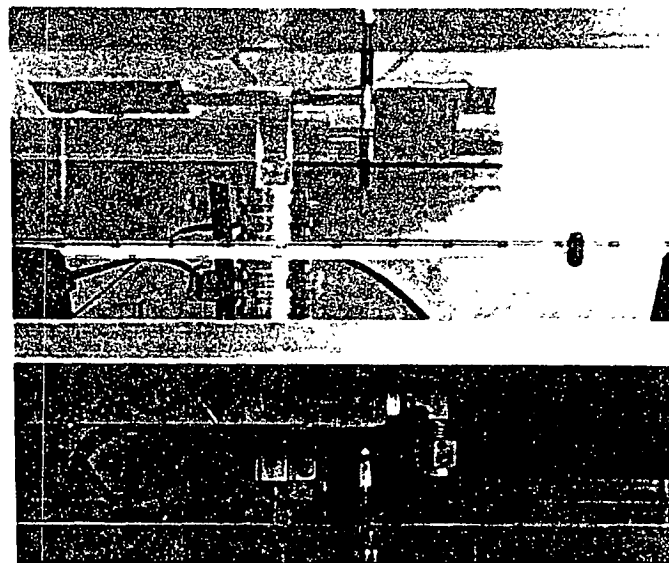


Fig. 11. Schematic of Thernonucleator showing growth cell, cold spot, cold spot temperature control and ambient temperature control by heat exchanger.



a)

ORIGINAL PAGE IS
OF POOR QUALITY



b)

Fig. 12. Thermonucleator apparatus showing
a) an overall view of the apparatus, and
b) a close-up of the upper portion.

ORIGINAL PAGE
BLACK AND WHITE PHOTOGRAPH

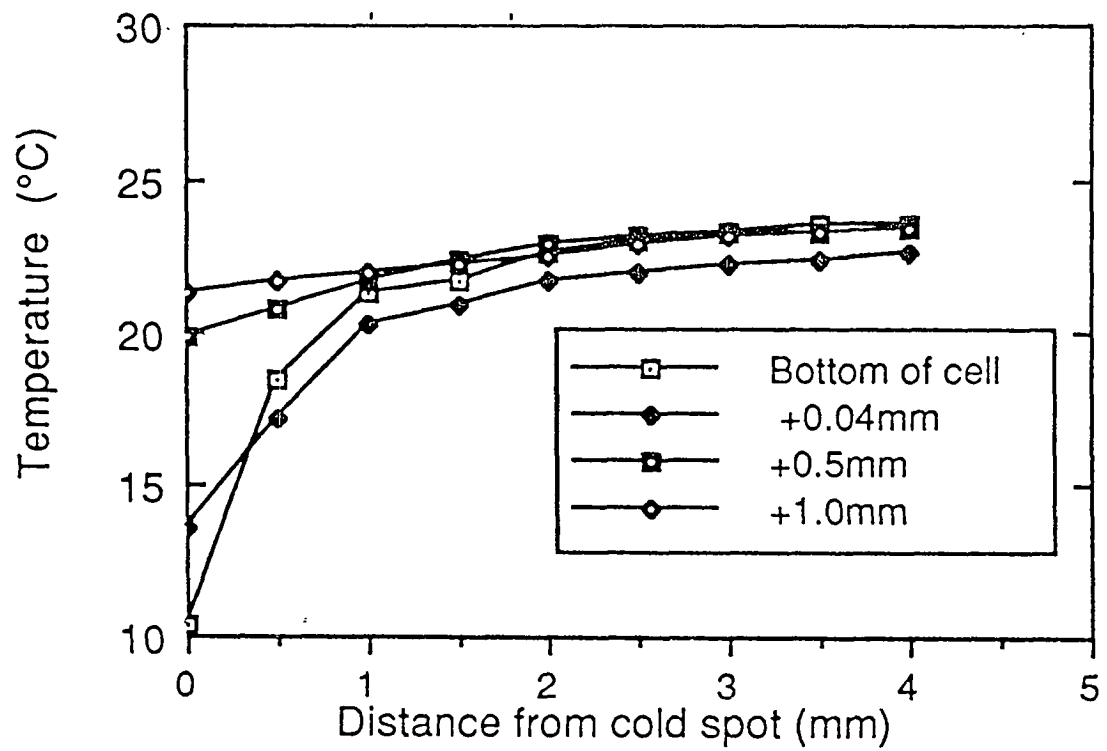


Fig. 13. Temperature gradients measured at various distances from the bottom of the growth cell in the Thermonucleator with a 25° C ambient and a 15° C cold spot.

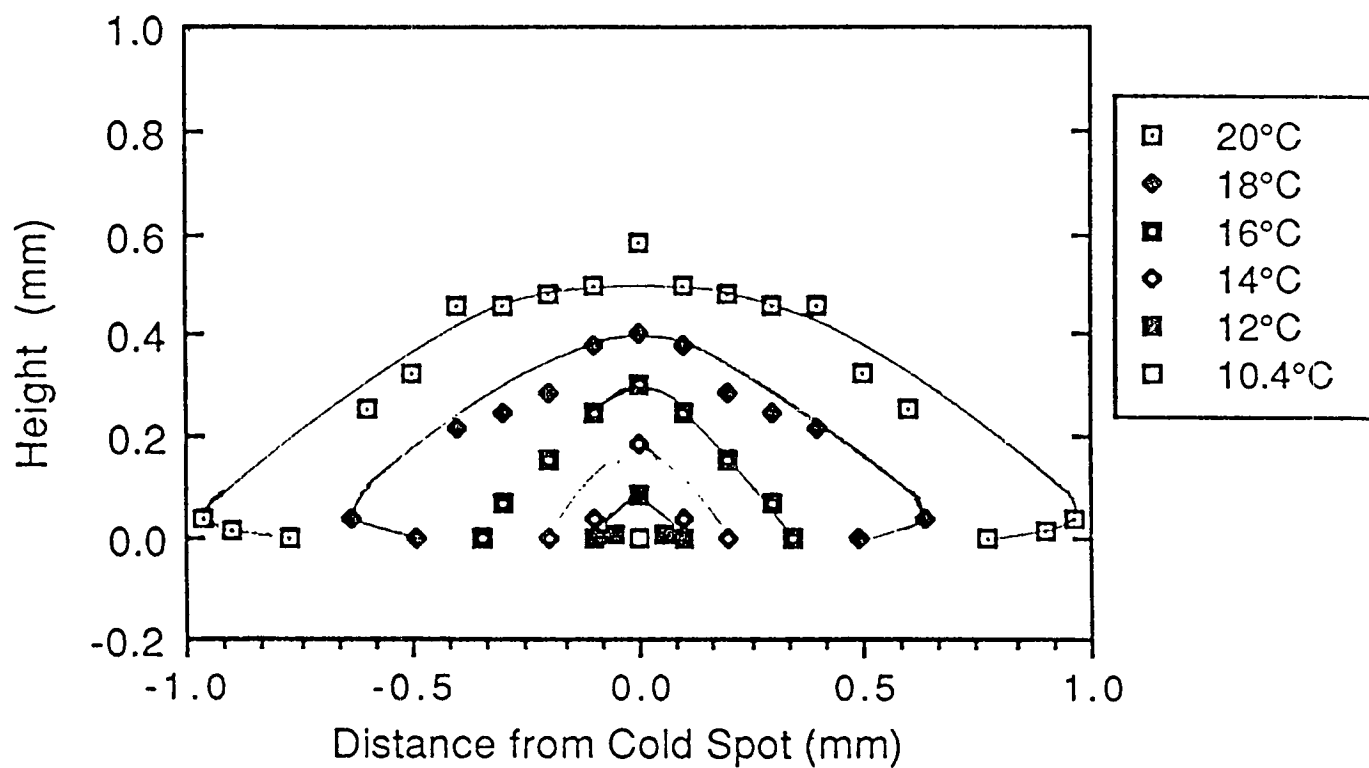


Fig. 14. Isotherms developed in growth cell of the Thermonucleator with a 25° C ambient and a 15° C cold spot.

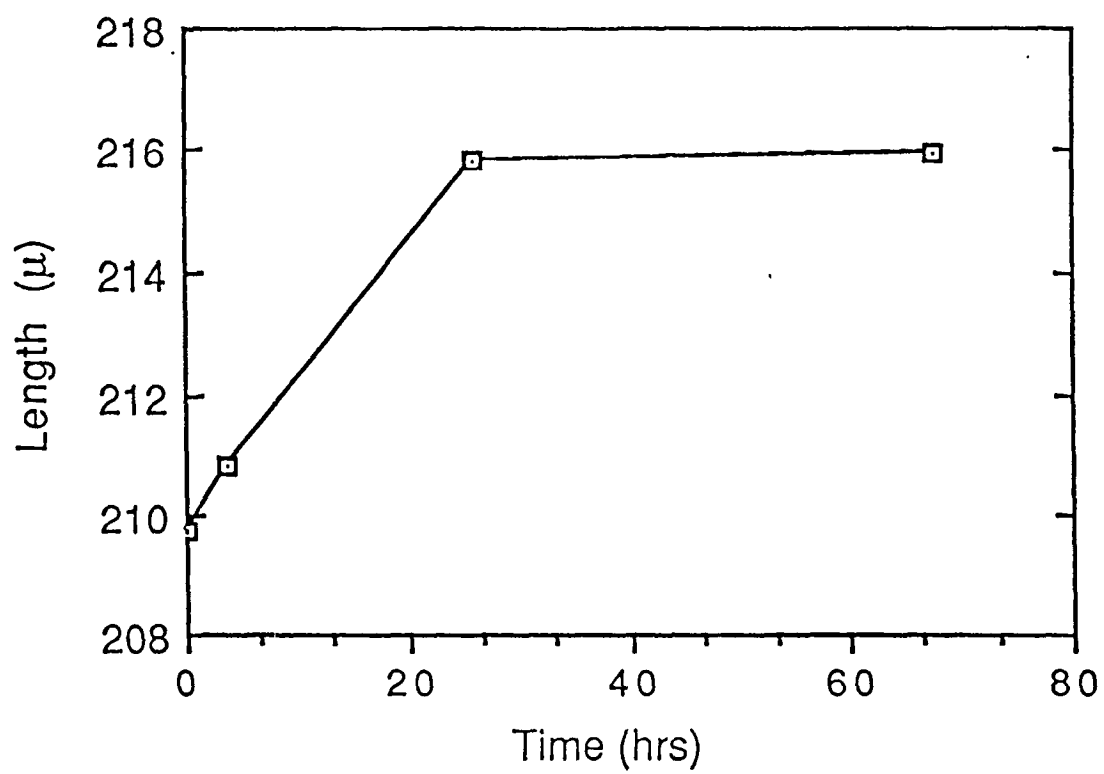
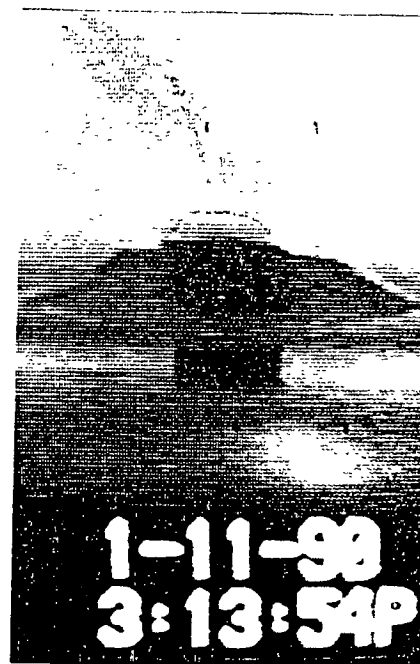
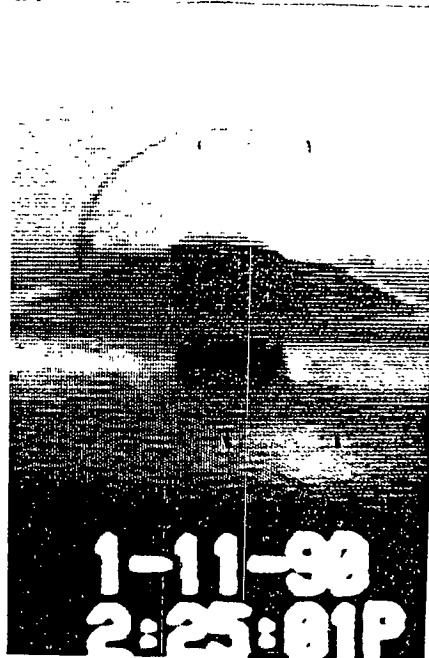
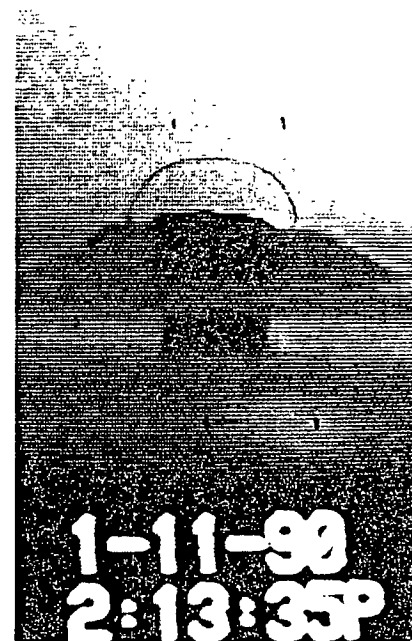
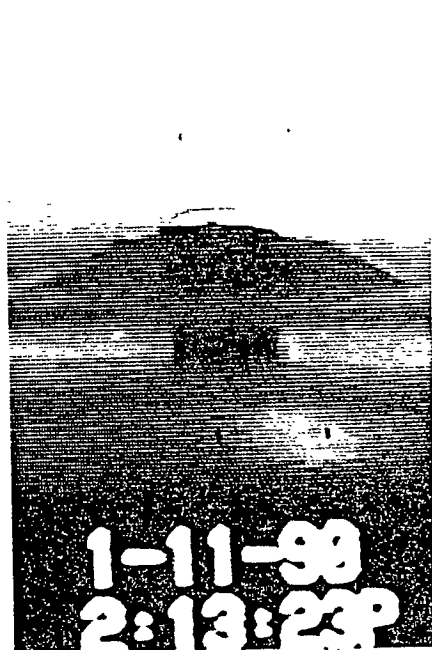


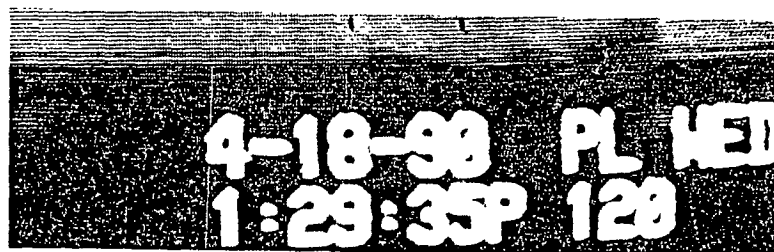
Fig. 15. Continued growth of a canavalin crystal when supersaturation was increased by lowering the temperature for 22 to 17° C.



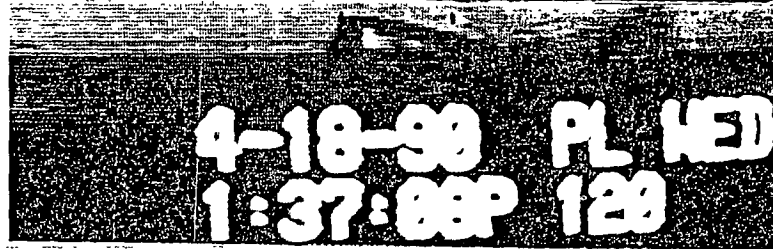
After melt back.

Fig. 16. Nucleation and growth of ice at 30° C ambient. Markers are 0.6mm.

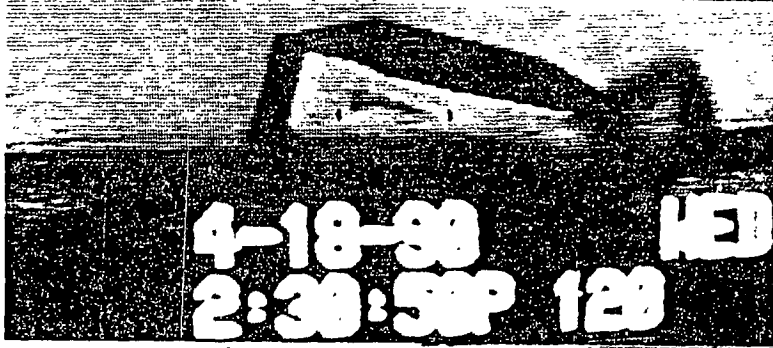
ORIGINAL PAGE IS
OF POOR QUALITY



$T_e = 24^{\circ}\text{C}$, $T_s = 16^{\circ}\text{C}$



$T_e = 24^{\circ}\text{C}$, $T_s = 16^{\circ}\text{C}$



$T_e = 22^{\circ}\text{C}$, $T_s = T_e$



$T_e = 20^{\circ}\text{C}$, $T_s = T_e$

Fig. 17. Nucleation and growth of Rochelle salt at 24°C (ambient, T_e) and cold spot temperature of 16°C (T_s). Starting solution was saturated at 24°C . Starting time was 11:11am. Markers are 0.6mm.

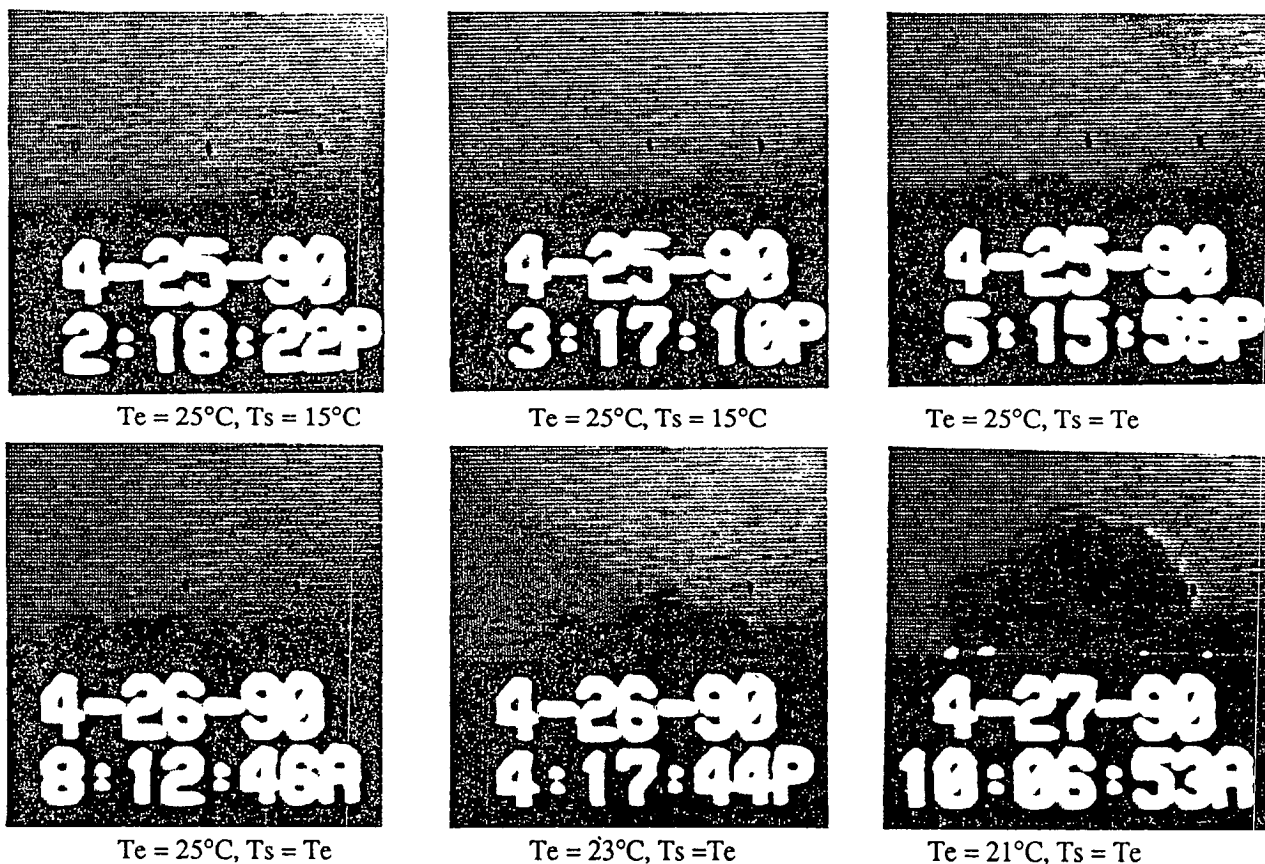


Fig. 18. Nucleation and growth of lysozyme at 25° C (ambient, Te) and cold spot temperature of 15° C (Ts). Starting solution was 58mg/ml of lysozyme at pH4 in 0.1M sodium acetate with 2% sodium chloride. Starting time was 9:49am. Markers are 0.6mm.

ORIGINAL PAGE IS
OF POOR QUALITY

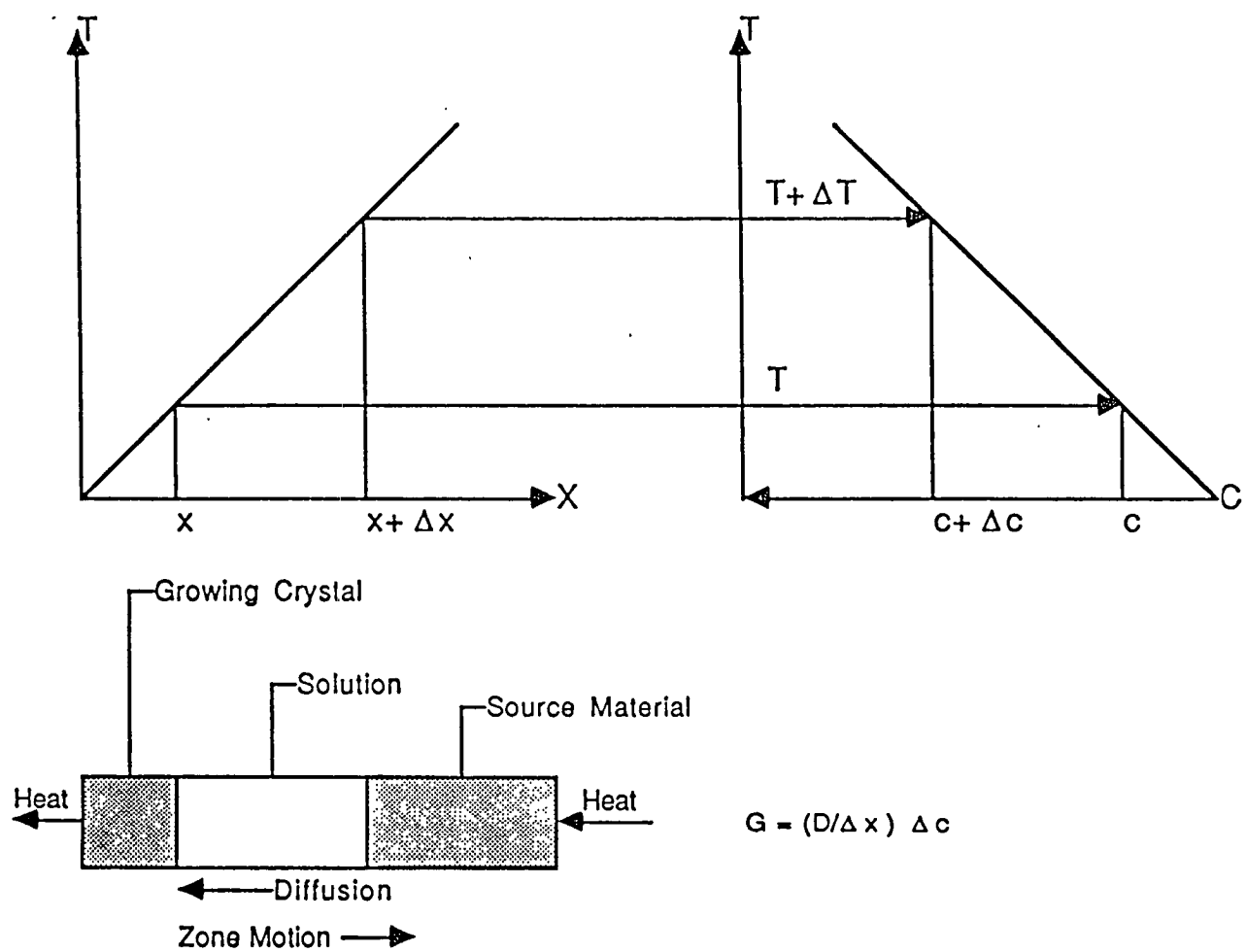


Fig. 19. Relationship between position, temperature and concentration in the temperature gradient growth technique. Inset shows directions of growth and diffusion.

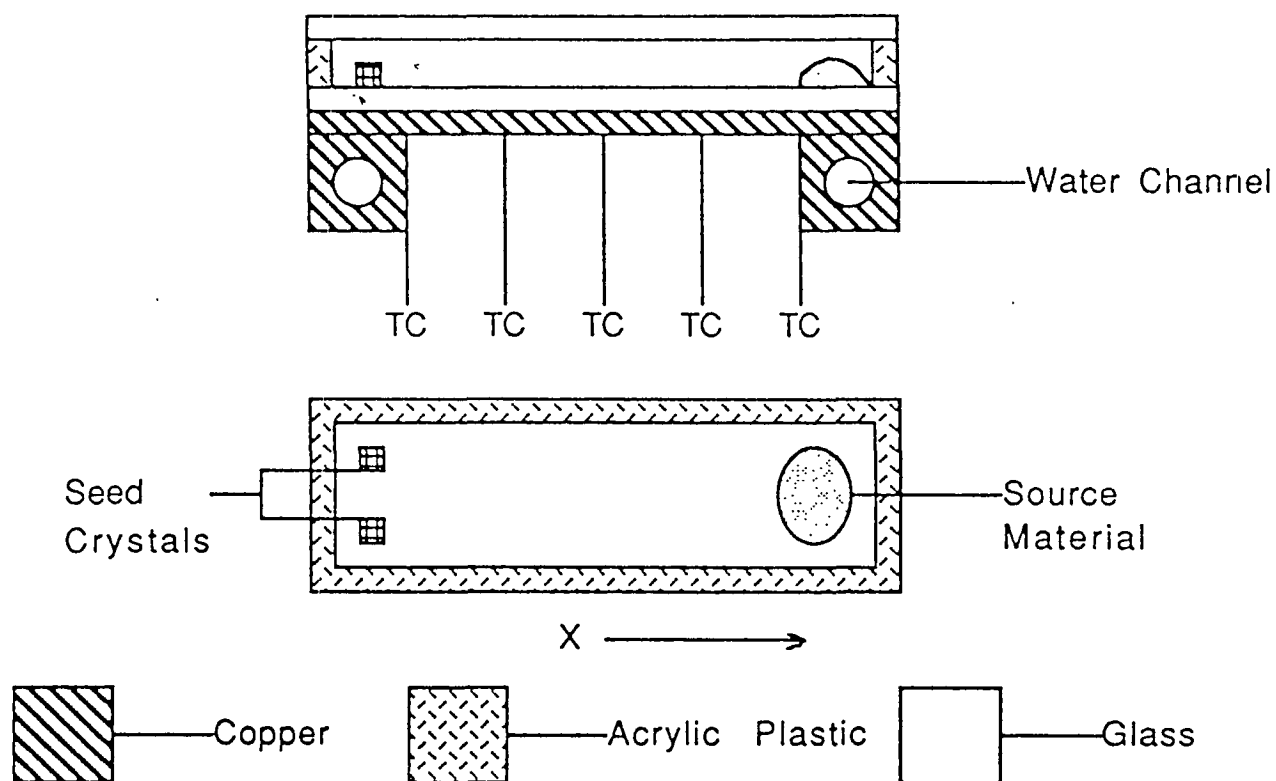


Fig. 20. Temperature gradient cell. Thermocouples are indicated by TC.

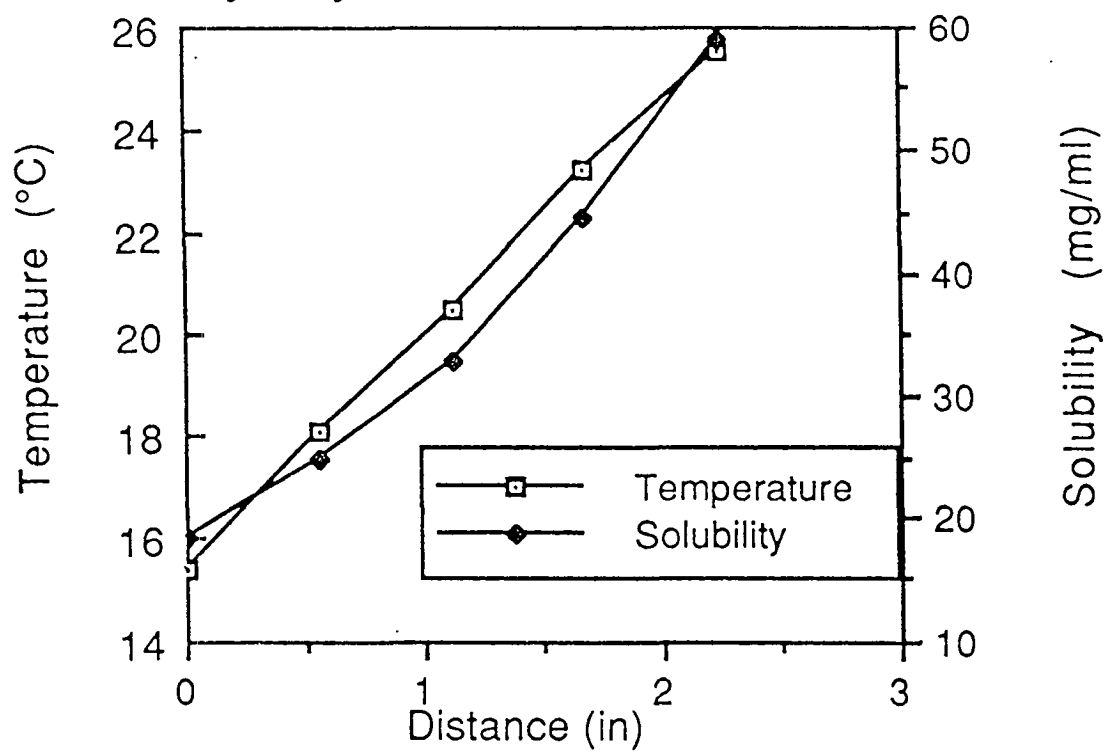


Fig. 21. Temperature and solubility gradients developed in temperature gradient cell.

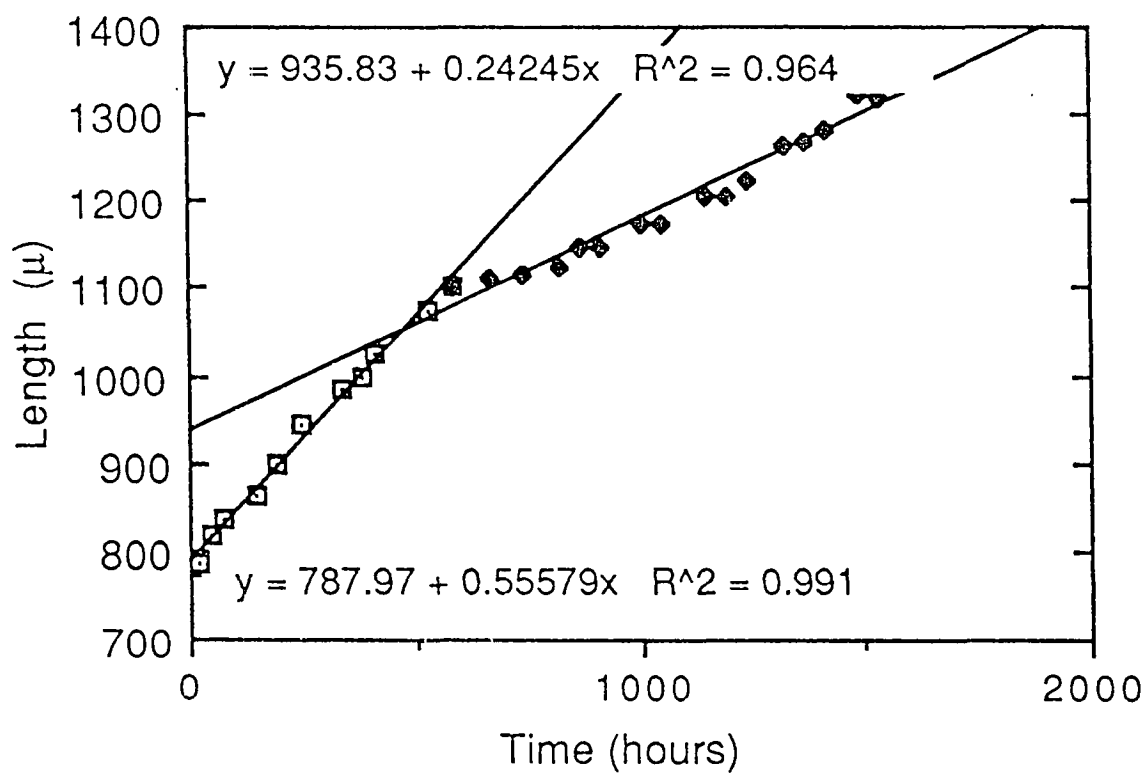
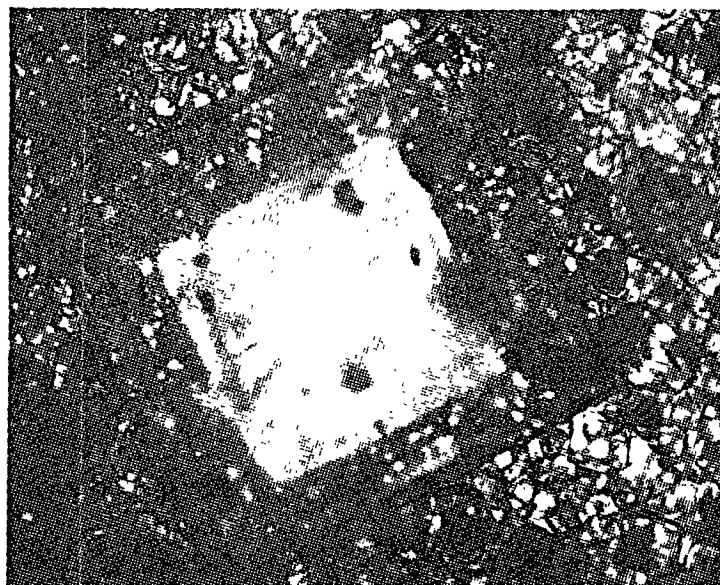
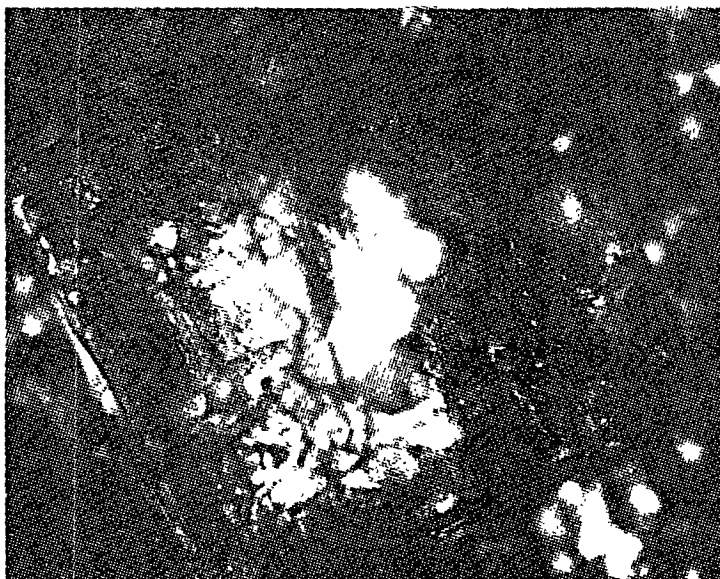


Fig. 22. Size versus time for a lysozyme crystal grown under the conditions of Fig. 21.

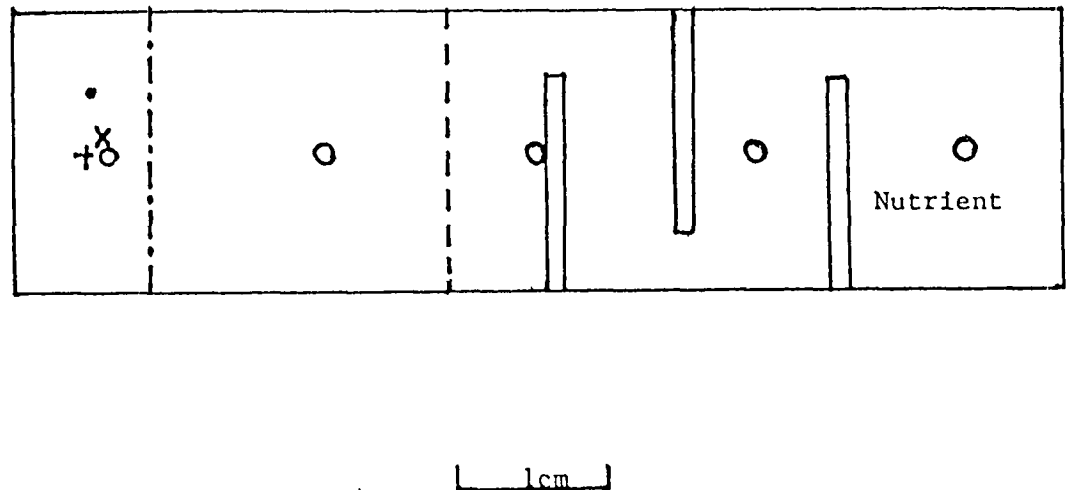


a)



b)

Fig. 23. Lysozyme crystal grown under conditions of Fig. 21 photographed in transmitted light with crossed polarizers.
 a) Secondary nucleation evident. Light area was the seed.
 b) Surface morphology developed during growth.
 Crystal size was 1320μ .



+ 900 μ 110 Crystal

X 110, 011 Crystal

• 600 μ 110 Crystal

○ Thermocouples

— — — — Boundary for > 50 μ crystals (secondary nucleation)

- . - . - Boundary - secondary nucleated crystals touch

Note: Small crystallites exist throughout right hand part of cell

Fig. 24. Baffled cell design to eliminate drift of source material.
Location of seeds, secondary nucleation and thermocouple
are indicated.

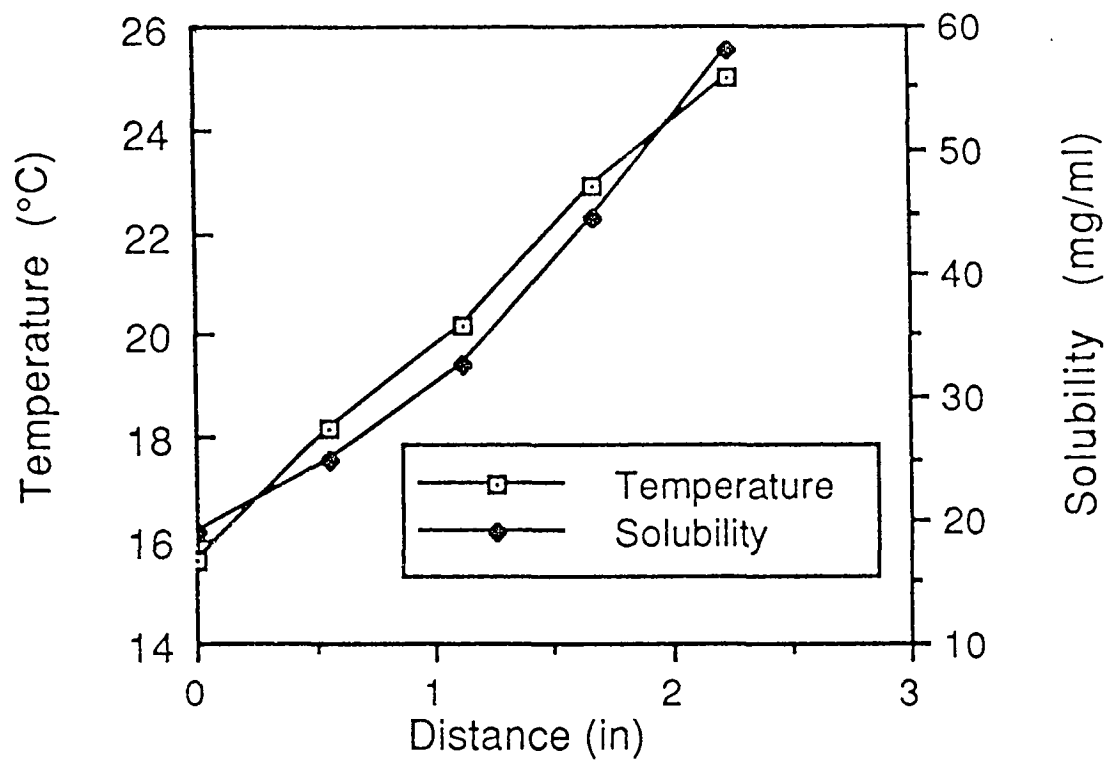


Fig. 25. Temperature and solubility gradients developed in baffled cell.

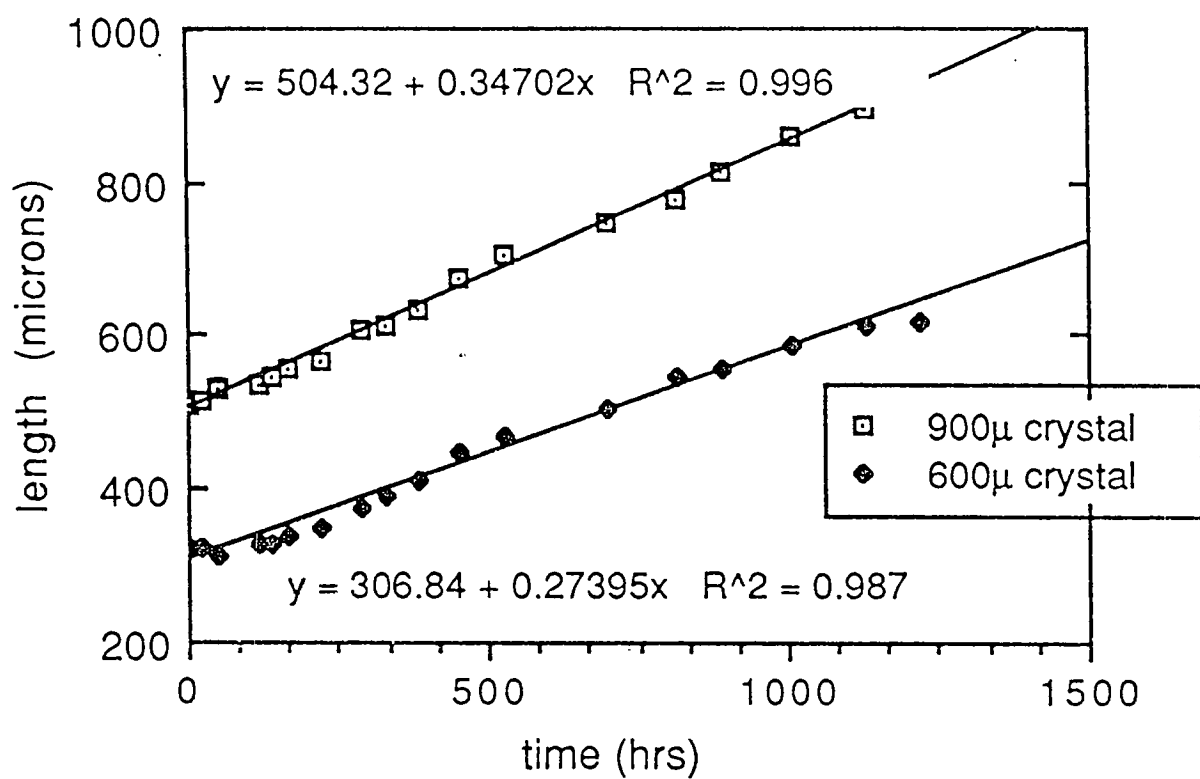


Fig. 26. Size versus time for lysozyme crystals grown under the conditions of Fig. 25.



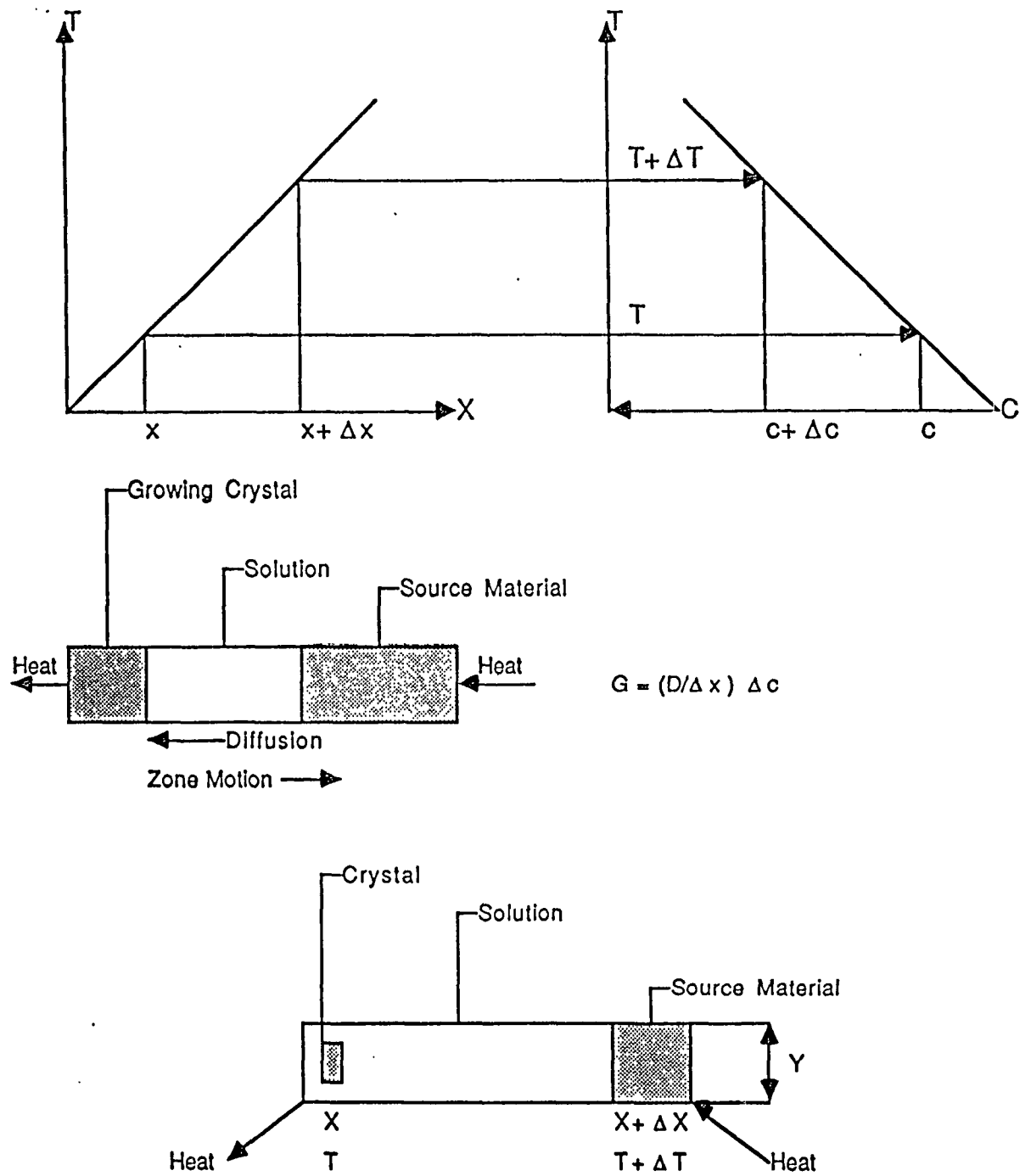
a)



b)

Fig. 27. Lysozyme crystals grown under the conditions of Fig. 25.
a) 922μ
b) 617μ .

ORIGINAL PAGE IS
OF POOR QUALITY



Variables: $X, Y, G, A, T, T + \Delta T, C, C + \Delta C$

Fig. 28. Parameters of temperature gradient growth technique.

